Large-Scale Synthesis of Metal Nanocrystals in Aqueous Suspensions
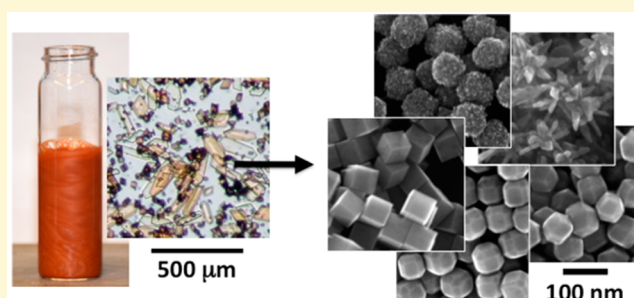
Anna Klinkova,[†] Egor M. Larin,[†] Elisabeth Prince,[†] Edward H. Sargent,[¶] and Eugenia Kumacheva[*,†]

[†]Department of Chemistry, University of Toronto, Toronto, Ontario M5S 3H6, Canada

[¶]The Edward S. Rogers Sr. Department of Electrical and Computer Engineering, University of Toronto, 10 King's College Rd, Toronto, Ontario M5S 3G4, Canada

ⓢ *Supporting Information*

ABSTRACT: Fundamental studies and practical use of metal nanoparticles (NPs) frequently depend on the ability to reproducibly synthesize large quantities of shape-specific NPs. For this reason, facile synthetic procedures are desired that will lead to large quantities of uniformly sized metal NPs exhibiting specific shapes. Here, we report a general approach to the large-scale synthesis of noble metal nanocrystals having well-defined shapes and a narrow size distribution. This method utilizes seed-mediated NP growth in aqueous suspensions of cationic surfactants and metal salts. It leads to a ~60-fold increase in NP volumetric production capacity, compared to

the most widely used solution-based synthetic methods. In addition, it uses up to 100 times less cationic surfactant than conventional solution-based methods. The applicability of the method is demonstrated in the synthesis of Pd nanocubes, rhombic dodecahedra, and polyhedrons with low index facets; branched Pd nanocrystals; alloy Pt/Pd nanocubes; Ag nanocubes. The advantages and limitations of the approach are discussed, including accessible shapes, growth kinetics, and the capability to scale up the synthetic procedure.

INTRODUCTION

Metal nanoparticles (NPs) exhibit optical, magnetic, and catalytic properties that are governed by NP size, shape, surface morphology, and surface chemistry, to name just a few important factors.[1] For example, the surface plasmon resonance properties of metal NPs depend strongly on their shape,[2] while NP catalytic performance depends on the facets, steps, kinks, and twin defects present on the NP surface.[3] The ability to alter NP properties by varying their size, shape, and structural characteristics paves the way for a variety of NP applications. Unfortunately, both fundamental studies and practical use of NPs are frequently hampered by the inability to synthesize reproducibly large quantities of shape-specific NPs.

Generally, the quantity of synthesized NPs is scaled up using a "numbering out" approach, that is, by carrying out parallel synthesis in a large number of identical small-scale reactors.[4] Recently, continuous microfluidic reactors have been used to scale-up the synthesis of micrometer and nanometer-size particles.[5,6] A different approach is based on increasing reaction volume;[7,8] however, nonuniform mixing and heat transfer in the reaction mixture often result in a broad size distribution of the resulting NPs and the appearance of shape impurities.

Alternatively, NP synthesis can be scaled up by increasing the concentration of the reactants to approach or even exceed their solubility threshold. When the solubility limit of precursor reagents is exceeded, the reaction takes place in a heterogeneous environment, in which solid-state precursors are used for continuous delivery of molecular precursors to the growing NPs.[9] The near and beyond the solubility limit

approaches have been proven effective for hot injection[9,10] and heat-up[11] synthesis of semiconductor NPs in nonpolar reaction medium; however, it remains unexplored for ionic surfactant-stabilized metal NPs that are synthesized in *aqueous* medium.

In addition to scaled-up synthesis, an important factor determining NP applications is the ability to remove or exchange ligands present on the surface of as-synthesized NPs. Currently, many methods of NP synthesis in either aqueous[12] or organic[13] media utilize polydentate poly(vinylpyrrolidone),[14] thiol-terminated molecules,[12,15] or aliphatic amines,[16] that is, the ligands that are strongly bound to the NP surface. The replacement of such ligands with other molecules in a ligand-exchange procedure is not trivial. On the other hand, cationic surfactants used in aqueous synthesis of metal NPs can be readily removed from the NP surface using, e.g., simple alcohols. Notably, the facile removal of such ligands due to their high solubility enables NP integration into various matrices and attachment to different substrates.[8] In addition, cationic surfactants, such as cetyltrimethylammonium bromide or cetylpyridinium chloride, are used in the synthesis of metal NPs with well-defined shapes that are generally not accessible when strongly bound ligands are used.[17,18] The majority of synthetic procedures involving cationic surfactant ligands have been reported for small (milliliter scale) reaction volumes with

a low concentration of the resulting metal NPs (less than 0.03 mg/mL).[18,19]

Thus, the development of scaled-up synthesis of shape-specific metal NPs in highly concentrated aqueous systems is highly desirable for efficient and sustainable production of NPs for a variety of applications. Here, we report a general methodology for the large-scale aqueous synthesis of cationic surfactant-stabilized metal NPs with a variety of shapes. In comparison with existing solution-based methods of NP synthesis, which rely on the use of cationic surfactants, we propose and prove an aqueous *suspension* approach. Our new strategy utilizes solid-state precursors in the liquid reaction mixture and a minimum amount of solvent. We utilized a high concentration of precursor reagents and developed a highly reproducible synthesis of shape-specific NPs in the quantity of up to 350 mg, which is ∼60-fold higher than NP quantity synthesized by conventional solution-based methods in the same reaction volumes.[18−21] Importantly, the proposed synthetic procedure is highly reproducible and requires 2 orders of magnitude less of a cationic surfactant than existing solution-based methods. Thus, the described synthetic method provides a greener approach to the synthesis of large batches of shape-controlled NPs for a variety of applications.

■ EXPERIMENTAL SECTION

Nanoparticle Synthesis. *Materials.* Ascorbic acid (98%), cetyltrimethylammonium bromide (CTAB, ≥99.0%), cetylpyridinium chloride (CPC, ≥99.0%), chloroauric acid (HAuCl$_4$, 99.99%), copper sulfate (CuSO$_4$·5H$_2$O, ≥98%), palladium dichloride (PdCl$_2$, 99%), sodium borohydride (NaBH$_4$, 98%), and sodium hexachloridoplatinate(IV) hexahydrate (Na$_2$PtCl$_6$·6H$_2$O, 98%) were purchased from Sigma-Aldrich. Hydrochloric acid (HCl, 36.5−38%) was purchased from Caledon Laboratories Ltd., silver nitrate (AgNO$_3$, ≥99.0%) was purchased from EMD Millipore, and sodium iodide (NaI, ≥99.5%) was purchased from AnalaR EM Science (Merck kGaA).

All aqueous solutions involving ascorbic acid, cetyltrimethylammonium bromide, cetylpyridinium chloride, chloroauric acid, palladium dichloride, silver nitrate, sodium borohydride, and sodium hexachloridoplatinate (IV) hexahydrate were freshly prepared before use. Deionized water was used throughout all the experiments.

Synthesis of Pd Nanocubes. Palladium nanocubes (NCs) were synthesized using a seed-mediated growth in aqueous Pd precursor suspension.

Step a: Synthesis of Seeds. Cube-shaped seeds were prepared using a previously reported procedure.[20] Briefly, to prepare 11 nm-size Pd cube-shaped seeds, 45.6 mg of cetyltrimethylammonium bromide (CTAB) was dissolved in 10 mL of deionized water in a 20 mL glass vial equipped with a stirring bar. The solution was heated to 95 °C under stirring, followed by the addition of 0.25 mL of 20 mM H$_2$PdCl$_4$ solution. After 5 min of stirring, 0.2 mL of 0.1 M ascorbic acid solution was quickly added. The reaction mixture was stirred for 10 min at 95 °C, then cooled down to 30 °C, and allowed to age for 1 h.

Step b: Seed-Mediated NC Growth in an Aqueous Suspension. A solution containing 1 g of CTAB in 6.8 mL of deionized water was mixed with 3.2 mL of 100 mM H$_2$PdCl$_4$ (obtained by mixing 57.5 mg of PdCl$_2$ with 3.25 mL of 0.2 M HCl under stirring for 3 h to obtain a clear orange-brown solution), resulting in the formation of a turbid orange suspension that was stirred in a water bath at 45 °C. Next, 10 mL of aged Pd cube-shaped seeds was added to the growth solution under vigorous stirring, followed by the addition of 5 mL of 1 M ascorbic acid. The resulting mixture was vigorously stirred at 45 °C for 6 h. The resulting Pd NCs solution was centrifuged at 5000*g* for 10 min at 27 °C to remove excess CTAB and was subsequently redispersed in deionized water. The same purification method was used for the other types of NPs, the synthesis of which is described below. The yield of NPs was nearly quantitative, except for minor

losses associated with the removal of the supernatant upon NPs centrifugation.

Pd Rhombic Dodecahedra and Pd Nanoparticles with Mixed Low Index Planes. Palladium rhombic dodecahedra (RDs) were obtained following the procedure described for Pd NCs; however in step (b), 0.25 mL of 10 mM NaI solution was added to CTAB solution prior to the addition of H$_2$PdCl$_4$. The optimized temperature for the RD growth was 30 °C, while at higher temperatures of up to 75 °C, the formation of RDs with mixed low index planes was observed. When a smaller amount of NaI was added, that is, 0.1 mL of 10 mM solution, truncated NCs were formed, instead of RDs, at reaction temperatures of 30−45 °C (see Figure S4 for the detailed [NaI]-temperature-shape correlation).

Pd Nanocubes with Protrusions. Palladium nanocubes with protrusions (PNCs) were synthesized following the procedure described for Pd NCs; however in step (b), 0.5 mL of 100 mM aqueous Cu$_2$SO$_4$ was added to the CTAB solution prior to the addition of H$_2$PdCl$_4$. The optimized temperature for the synthesis of well-defined BNPs was in the range of 30−45 °C.

Branched Pd Nanoparticles. Branched palladium NPs (BNPs) were synthesized using a seed-mediated growth in aqueous Pd precursor suspension.

Step a: Synthesis of Seeds. Polygonal seeds were prepared using a previously reported procedure.[21] Briefly, 345 mg of CTAB was mixed with 10 mL of 0.25 mM solution of Na$_2$PdCl$_4$ in a 50 mL two-neck round-bottom flask equipped with a stirring bar; the solution was bubbled with nitrogen for 30 min at 30 °C. Then, 0.22 mL of freshly prepared ice-cold NaBH$_4$ aqueous solution was injected into the reaction mixture under vigorous stirring, resulting in the formation of ∼3 nm of preseeds. This solution was maintained under a nitrogen atmosphere to prevent dissolution of the preseeds due to oxidation. Next, 690 mg of CTAB and 20 mL of a 0.25 mM solution of Na$_2$PdCl$_4$ were mixed in a 20 mL vial, followed by the addition of 156 μL of 0.1 M ascorbic acid and 168 μL of preseed solution to form polygonal Pd NPs that were used to grow BNPs. The vial was shaken for 5 s and left to age for 2 h.

Step b: Seed-Mediated Growth of BNPs in an Aqueous Suspension. The growth of BNPs was performed as described for Step b of the synthesis of Pd NCs; however, 1 mL of 100 mM Cu$_2$SO$_4$ was added to the CTAB solution prior to the addition of Na$_2$PdCl$_4$, and 10 mL of polygonal Pd seeds were used in the place of cubic Pd seeds.

Pd/Pt Nanocubes. Pd−Pt 1:1 alloy NCs were synthesized following the procedure described for the synthesis of Pd NCs; however in step (b), a mixture of 1.6 mL of 100 mM H$_2$PdCl$_4$ and 1.6 mL of 100 mM Na$_2$PtCl$_6$ was used in place of 3.2 mL of the 100 mM H$_2$PdCl$_4$ solution.

Ag Nanocubes. Pd-seeded Ag NCs were synthesized using the procedure described for the synthesis of Pd NCs; however in step (b), CTAB was substituted with an equimolar amount of CPC, and 2.5 mL of 150 mM AgNO$_3$ was used in place of H$_2$PdCl$_4$.

Nanoparticle Characterization. Scanning and transmission electron microscopy (SEM and TEM, respectively) imaging was performed using a Hitachi S-5200 microscope operating at 25 kV and equipped with an EDX detector. Samples for imaging were prepared by depositing a droplet of NP solution on a 400 mesh carbon-coated copper grid and allowing the solvent to evaporate.

For NP shape-purity analysis, at least, five different areas on the SEM grid were analyzed by counting the NP with the predetermined, desired shapes, as well as the NPs with other shapes. The total number of NPs was at least 300. The ratio of the number of NPs with the desired shape to the total number of NPs was defined as shape purity.
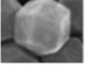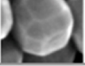
For NP size analysis, the dimensions of at least 200 NPs were measured using ImageJ. The size was defined as an average side length of a cube for Pd, Pd/Pt, and Ag NCs, while for other NP types, it was defined as an average diameter of a circle that can fit a NP. Shape purity and size distribution histograms are shown in Figures S13−S18.

Optical microscopy was performed using an optical microscope Nicon D7200. Extinction spectra of Ag NCs were acquired using a Cary-5000 UV−vis-NIR spectrophotometer.

■ RESULTS AND DISCUSSION

The large-scale synthesis of metal NPs relied on continuous supply of precursor molecules via gradual dissolution of the solid precursor microparticles present in the reaction mixture. Being motivated by the utilization of Pd NPs in catalysis[22,23] and chemical[24,25] and biological[26,27] sensing, as well as hydrogen storage,[28,29] we examined in detail the proposed synthetic methodology for the large-scale synthesis for Pd NPs. The versatility of the method was further demonstrated by synthesizing NPs of other noble metals, namely, Ag and Pd/Pt alloy NCs. Table 1 shows the summary, notations, and

Table 1. NPs Synthesized Using the Suspension Approach

Pd-seeded NPs	Cartoon	SEM image	Dimensions[a], nm	Shape purity, %
Pd nanocubes (Pd NCs)			37±4	97%
Pd rhombic dodecahedra (Pd RDs)			71±6	96%
Pd NP with mixed low index facets			67±6	95%
Pd nanocubes with protrusions (Pd PNCs)			30±3	60%
Pd branched NPs (Pd BNPs)			108±11	95%
Pd/Pt (1:1) alloy nanocubes (Pd/Pt NCs)			56±6	78%
Ag nanocubes (Ag NCs)			45±4	73%

[a]For Pd, Pd/Pt, and Ag NCs, dimensions correspond to the side length of a cube. For all other NP types, dimensions correspond to the diameter of a sphere fitting a NP.

characteristics for the NPs synthesized by the proposed suspension approach. The synthetic procedure was highly reproducible: for each type of NPs, the synthesis was repeated at least 6 times and yielded NPs with narrow size distribution and high shape purity.

Synthesis of Pd Nanocubes. In a well-established solution-based protocol of seed-mediated secondary growth of Pd NCs,[18] reduction of Pd^{2+} on the surface of 10−20 nm-size Pd cubic seeds occurs in an aqueous 0.05−0.1 M CTAB solution containing 0.25 mM H_2PdCl_4 and ascorbic acid. In our work, we found that Pd NCs can form at a 50-fold increase in concentration of H_2PdCl_4 (that is, 12.5 mM), Pd seeds, and ascorbic acid in 0.1 M aqueous CTAB solution (see Figure S1).

Mixing of H_2PdCl_4 and CTAB solutions in such a high concentration regime yielded a turbid orange-color suspension of particles with dimensions in the range from 2 to 200 μm (Figure 1a,b,b′). The analysis of the chemical composition of these microscopic crystals by energy-dispersive X-ray spectroscopy (EDX) revealed the presence of Pd, Cl, and Br (Figure 1g−j) at elemental ratios of Pd/Cl/Br = 3:2:5. Most likely, these crystals were formed due to ionic interactions between the cationic CTAB and the negatively charged $PdCl_4^{2-}$ complex. We speculate that poor solubility of these crystals in water was caused by the high $PdCl_4^{2-}$ concentration and the presence of the hydrophobic tail of cationic surfactants emanating from the surfactant−complex adduct. The key contribution of the surfactant to the formation of the microscale crystals was confirmed by the fact that they did not form in the reagent solution with an equivalent concentration of KBr introduced instead of CTAB. The formation of the suspension of micrometer-size crystals, as opposed to a solution, was observed when the concentration of H_2PdCl_4 exceeded 5 mM. Later in the text, we refer to the suspension containing precursor aggregates as a "growth suspension".

Upon addition of the cube-shaped Pd seeds and ascorbic acid to the Pd growth suspension, the latter gradually changed its color from orange to black and the microcrystals reduced their
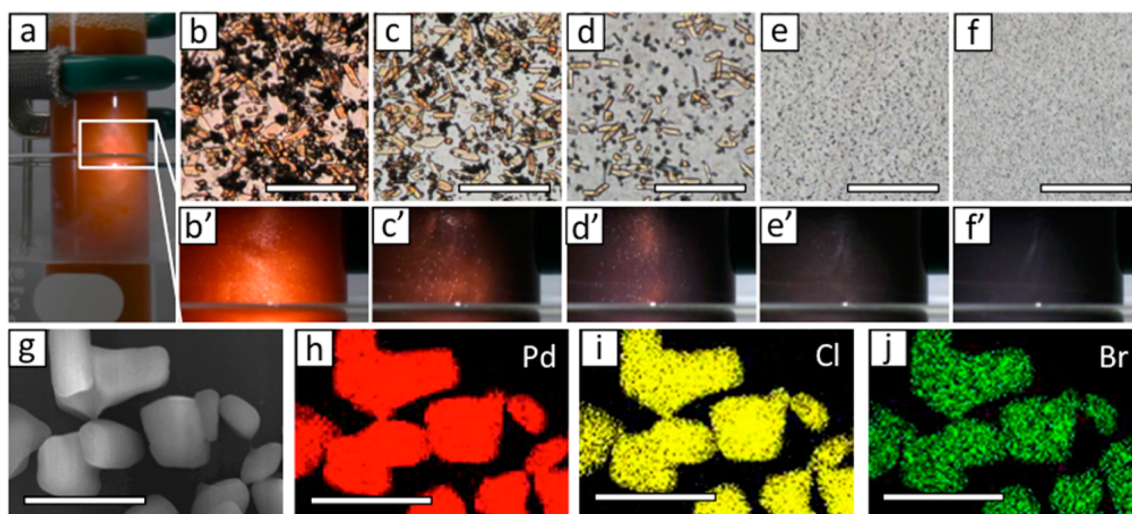
Figure 1. Changes in the reaction mixture during the first 90 min for Pd NCs growth at 12 mM Pd^{2+} concentration. (a) Photograph of the reaction mixture in a 30 mL vial. (b−f) Optical microscopy images of the reaction mixture at the beginning of the reaction (a) and after 30 (c), 45 (d), 60 (e), and 90 (f) min. The scale bars in (b−f) are 500 μm; corresponding photographs of the solution mixture are shown in (b′−f′). SEM image of the collected precipitate from the reaction mixture after 30 min with no stirring (g) and corresponding EDX maps of Pd (h), Cl (i), and Br (j); scale bars are 10 μm (g−j).

size over the course of 90 min at 45 °C (Figure 1b−f and b′−f′). After 2 h, the microcrystals completely dissolved. This change was accompanied by the progression of Pd NC growth, as Pd^{2+} was reduced on the surface of Pd seeds, thus decreasing the concentration of Pd^{2+} in the solution. After 3 h, a black colloidal solution of Pd NCs was formed (Figure 2a). We note
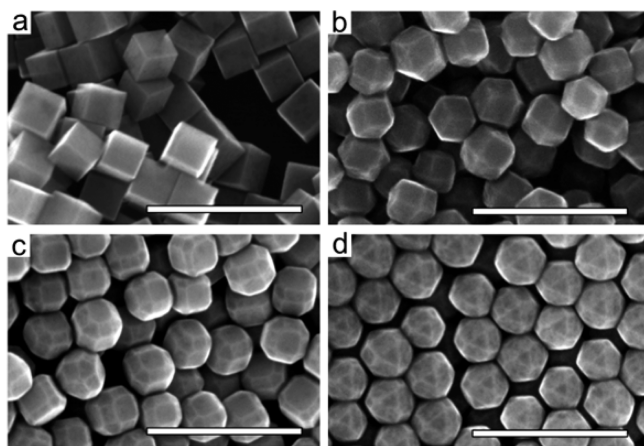
Figure 2. SEM images of Pd nanoparticles synthesized using a suspension method with no inorganic ion additives (a) and in the presence of I^- ions: $[I^-]$ = 0.1 mM at 30 °C (b), $[I^-]$ = 0.05 mM at 30 °C (c), and $[I^-]$ = 0.1 mM at 45 °C (d). Scale bars are 200 nm.

that, unlike the low-concentration solution-based synthesis of Pd NCs, in which the reaction mixture is typically left undisturbed, in the suspension-based method, stirring of the reaction mixture was critically important. If the stirring stopped, the microscopic crystals settled, while the Pd NC growth continued, thereby yielding polydisperse Pd nano- and microscopic cubes and rectangular prisms, likely resulting from the merge and subsequent overgrowth of Pd NCs trapped in the sediment (Figure S2). In the course of experiments, we found out that high shape purity and narrow size distribution of Pd NCs with standard deviation less than 10% was achieved in reactions performed in vials with a volume up to 30 mL and in the round-bottom flask with a volume up to 250 mL under magnetic stirring, thus yielding 350 mg of Pd NCs.

Further >60-fold increase in the concentration of Pd seeds and $PdCl_4^{2-}$, in comparison with conventional solution-based Pd NC synthesis, corresponding to $\left[PdCl_4^{2-}\right] \geq 15$ mM in the growth suspension, resulted in the formation of polydispersed Pd NCs and the increasing fraction of shape impurities. This effect could be caused by reaching the threshold Pd^{2+}/CTAB ratio, with an insufficient amount of CTAB to form a stable bilayer around each growing Pd NC, thus causing their aggregation and overgrowth. A similar effect was observed when the concentration of CTAB in the growth suspension was decreased by a factor of 2 (Figure S3).

Upon addition of the cube-shaped Pd seeds and ascorbic acid to the Pd growth suspension, the latter gradually changed its color from orange to black and the microcrystals reduced their size over the course of 90 min at 45 °C (Figure 1b−f and b′−f′). After 2 h, the microcrystals completely dissolved. This change was accompanied by the progression of Pd NC growth, as Pd^{2+} was reduced on the surface of Pd seeds, thus decreasing the concentration of Pd^{2+} in the solution. After 3 h, a black colloidal solution of Pd NCs was formed (Figure 2a). We note that, unlike the low-concentration solution-based synthesis of

Pd NCs, in which the reaction mixture is typically left undisturbed,[18] in the suspension-based method, stirring of the reaction mixture was critically important. If the stirring stopped, the microscopic crystals settled, while the Pd NC growth continued, thereby yielding polydisperse Pd nano- and microscopic cubes and rectangular prisms, likely resulting from the merge and subsequent overgrowth of Pd NCs trapped in the sediment (Figure S2). In the course of the experiments, we found out that high shape purity and narrow size distribution of Pd NCs with a standard deviation of less than 10% was achieved in reactions performed in vials with a volume up to 30 mL and in the round-bottom flask with a volume up to 250 mL under magnetic stirring, thus yielding 350 mg of Pd NCs.

Further >60-fold increase in the concentration of Pd seeds and $PdCl_4^{2-}$, in comparison with conventional solution-based Pd NC synthesis,[18] resulted in the increasing fraction of shape impurities and a broader size distribution of Pd NCs. This effect could be caused by reaching the threshold Pd^{2+}/CTAB ratio, with an insufficient amount of CTAB to form a stable bilayer around each growing Pd NC, thus causing NC aggregation and overgrowth. A similar effect was observed when the concentration of CTAB in the growth suspension was decreased by a factor of 2 (Figure S3).

Effect of Anionic Additives. Generally, addition of inorganic anionic additives to growth solutions allows for the controlled growth of nanocrystals with specific shapes due to the preferential binding of particular ions to specific facets.[22] For example, Pd NPs typically assume a cubic shape, when grown in CTAB solutions, because Br^- ions of CTAB preferentially attach to {100} facets.[31] We explored the effect of addition of I^- ions, which stabilize {100} and {111} facets in Pd nanocrystals,[18] on the shape of Pd NPs synthesized using a growth suspension approach. We added a different amount of I^- ions to the growth suspension described in the previous section. As the relative stability of {100} and {111} facets depends on the reaction temperature,[18] we explored the effect of the addition of $[I^-]$ ions in the temperature range from 30 to 90 °C. While in the absence of I^- ions, the NCs were formed in the entire temperature range studied, and with an increase in the concentration of I^- ions at temperatures of 30−75 °C, the resulting NPs changed their shape from cubes to truncated cubes, to truncated rhombic dodecahedra, and finally to rhombic dodecahedra (Figure 2).

At reaction temperatures below 75 °C, an increase in $[I^-]$ beyond 0.1 mM led to the formation of rhombic dodecahedra with ill-defined {110} planes. At higher temperatures, truncated cubes with smeared edges were formed. The formation of NPs with well-developed edges shown in Figure 2 was favored at 30−45 °C, while at the temperature above 60 °C the NP edges were smeared. Figure S4 illustrates NP shapes in the broad range of $[I^-]$ and temperatures.

On the basis of these results, we conclude that selective stabilization of {110} facets and consequent synthesis of RDs can be achieved in the growth suspension method. In addition, we explored the possibility of synthesizing Pd NPs with different fractions of low-index facets (Figure 2c,d). Figure S4 shows the relationship between the reaction parameters and NP shapes. We found however that the formation of Pd octahedra NPs enclosed solely by less thermodynamically stable {111} facets was not accessible via the described method, in contrast with a traditional low-concentration procedure, in which these

NPs can be obtained at 30−45 °C, albeit with ill-defined {111} facets.[18]

Effect of Cationic Additives. It is established that the introduction in the growth solution of cations of a second metal (with a reduction potential distinct from the main metal used for NP synthesis) promotes the development of high index NP facets.[18−34] Common examples of this phenomenon include the addition of Ag^+ or Cu^{2+} to the growth solutions of Au and Pd NPs, favoring the formation of elongated edges or branches. This effect is attributed to the underpotential deposition of the foreign metal on the edges and protrusions of the growing NP.[21] To examine whether this effect is applicable to the NP synthesis in high-concentration aqueous precursor suspension, we added Cu^{2+} ions at $[Cu^{2+}] = 2$ mM in the reaction mixture used for the synthesis of Pd NCs. Indeed, we observed the formation of Pd NCs with small protrusions (PNCs) at the NC corners and edges (Figure 3a); however, these protrusions were
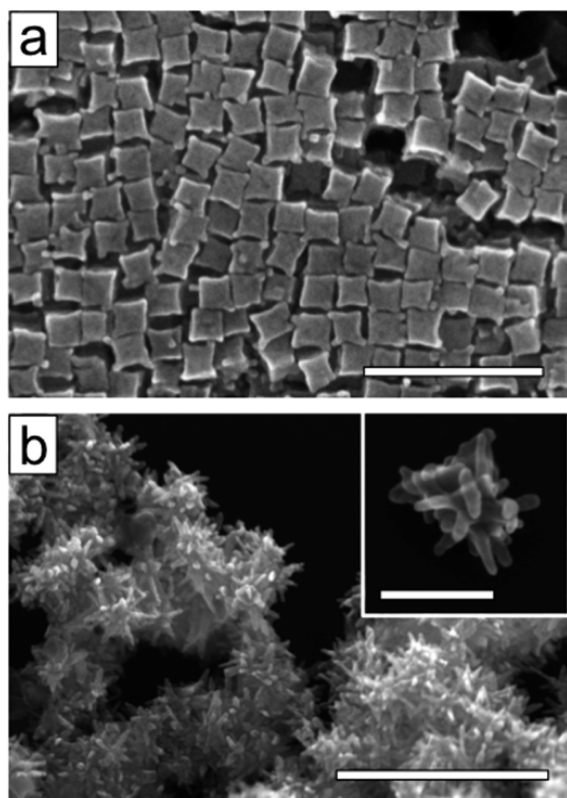

Figure 3. SEM images of PdCu NPs synthesized in the presence of Cu^{2+} ions on cubic seeds ($[Cu^{2+}] = 2$ mM) (a) and polyhedra-shaped seeds ($[Cu^{2+}] = 5$ mM) (b). Scale bars are 200, 500, and 100 nm in (a), (b), and (b inset) respectively.

ill-defined, in comparison with the structures reported for the corresponding low-concentration synthesis.[35] At $[Cu^{2+}] = 5$ mM, we observed the formation of a nearly 1:1 mixture of ill-defined protruded nanocubes and branched NPs (Figure S5).

To explore the effect of seed shape on the shape of the resulting NP in the presence of Cu^{2+} ions, we used polygonal Pd seeds (Figure S6), instead of cubic Pd seeds (see Experimental Section for synthetic details). Due to the presence of many edges on the polygonal seeds, multiple branches were grown on the seed surface in the presence of Cu^{2+} ions, resulting in highly branched NPs (BNPs, Figure 3b). Interestingly, due to the significantly higher total surface area

of branched NPs than the total surface area of other Pd NPs, due to the lack of CTAB, the resulting BNPs tend to aggregate. However, upon dilution of the NP solution with 0.1 M CTAB solution and subsequent sonication, they formed a colloidally stable solution.

While in low-concentration solution-based synthesis at low concentration of Cu^{2+} ions, Pd nanorods with a high aspect ratio grew on the surface of polygonal Pd seeds,[36] and in the concentrated suspension method described herein, we did not observe the formation of Pd nanorods at a considerable yield at $[Cu^{2+}]$ varying from 0 to 5 mM. More specifically, in the absence of Cu^{2+} ions, Pd polygonal seeds grew into a mixture of polydisperse polygonal NPs with a small fraction of small aspect ratio nanorods (Figure S7). At $[Cu^{2+}] < 5$ mM, we observed the formation of Pd BNPs. At $[Cu^{2+}] > 5$ mM, the reaction mixture gelled. Importantly, according to the EDX analysis, the fraction of Cu incorporated in the Pd BNPs was up to 20% (corresponding to 1:4 atomic ratio Cu/Pd), while in the low-concentration solution-based approach, we only detected up to 8% of Cu in the NPs at the same initial ratios of the $[Cu^{2+}]/[Pd^{2+}]$ precursors (of up to 2:5).

Synthesis of Ag and Pt/Pd NPs. To demonstrate the versatility of the growth suspension method, in addition to Pd NPs, we synthesized NCs of other noble metals. More specifically, we explored the applicability of the suspension growth approach to the synthesis of Pd-based alloy NCs and Ag NCs grown on either Pd or Au seeds (Table 1).

Generally, for alloy NPs with similar reduction potentials of the constituent metals, the NP shape is affected by the preferential anionic stabilization of specific facets of the metals. For the synthesis of Pd/Pt alloy NCs with 1:1 elemental ratio, we replaced $PdCl_4^{2-}$ with $[PdCl_4^{2-}]/[PtCl_6^{2-}]$ (1:1 mixture) in the protocol described in the Experimental Section. While the overall shape of the resulting Pd/Pt alloy NPs was cubic (Figure 4a), the surface of the NPs was rough, similar to the surface of spherical Pt NPs obtained in the reduction of Pt in the Pt-only growth suspension (Figure S8). The appearance of surface roughness was consistent with the previously reported
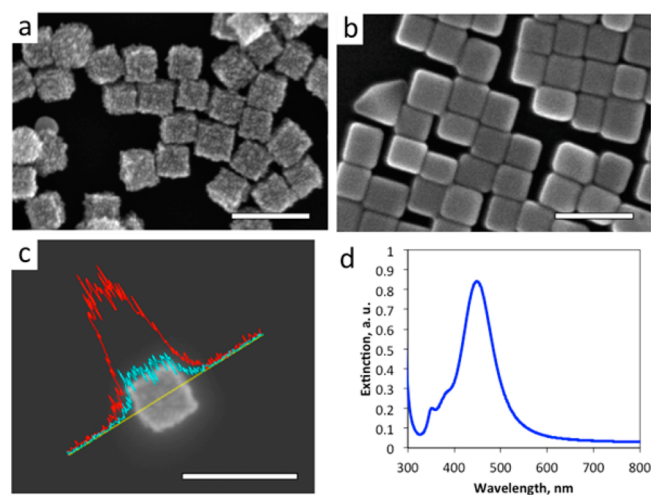

Figure 4. Pt/Pd alloy and Ag NCs synthesized using the suspension approach using 11 nm Pd cubic seeds. (a,b) SEM images of Pd/Pt alloy NCs (a) and Ag NCs (b). (c) EDX line scan of an individual Pd/Pt NC showing Pd (red) and Pt (blue). Elemental composition was ~1:1 by EDX. All scale bars are 100 nm. (d) UV−visible spectra of plasmonic Ag NCs.

synthesis of Pt NPs in the presence of cationic surfactants.[37] The formation of an alloy was confirmed by EDX analysis (Figure 4c).

Furthermore, since in the synthesis of Ag NCs, Cl^- ions stabilize Ag {100} facets,[37] we utilized the suspension approach described in the Synthesis of Pd Nanocubes; however, we replaced CTAB with CPC and used Ag^+ precursor in place of Pd^{2+}. The resulting Ag NCs had ∼10% of shape impurities. In the extinction spectrum of Ag NC solution, we observed a narrow surface plasmon resonance peak centered at 450 nm with shoulder peaks at 350 and 380 nm, which are characteristic of Ag NPs with cubic shape (Figure 4d).[37,38] Similarly, Ag NCs were synthesized by using 3−5 nm Au seeds, instead of utilizing Pd seeds, though the shape purity was compromised, possibly due to the less-defined, polygonal shape of small Au seeds (Figure S9). Interestingly, the stability of Ag NCs synthesized using a high-concentration suspension approach was decreased, in comparison with the low-concentration solution method, with NCs merging within hours after the synthesis. This effect may originate from insufficient surface stabilization coupled with daylight exposure of Ag NCs. Indeed, conducting the synthesis and storing Ag NCs in the dark extended their shelf life to several days.

CONCLUSION

We developed a large-scale aqueous suspension-based method for the synthesis of metal NPs stabilized with cationic surfactants. The method enables up to a 60-fold increase of the concentration of NPs in the reaction mixture, compared to conventional solution-based synthesis of metal NPs stabilized with cationic surfactants. As a result, up to 350 mg of metal NP with high shape purity and narrow size distribution can be produced. The versatility and generality of the approach was demonstrated by synthesizing Pd NPs with various shapes, including nanocube, rhombic dodecahedron, NPs with mixed low index facets, nanocubes with protrusions, and branched NPs, as well as Ag and alloy Pt/Pd NCs.

We reduced the amount of solvent and consumption of cationic surfactants by up to 2 orders of magnitude, in comparison with conventional solution-based synthesis. Thus, the described synthetic method provides a greener approach to the synthesis of large batches of shape-controlled NPs for a variety of applications.

Importantly, the synthetic procedure was highly reproducible and could be handled by undergraduate students (E.M.L. and E.P.) without reducing shape purity and broadening NP size distribution. We expect that the synthetic procedure reported in the present work can be adapted in large-volume batch reactors with a design providing sufficient mixing. Alternatively, large-scale suspension-based synthesis of metal NPs can be conducted in continuous microfluidic flow reactors.

ASSOCIATED CONTENT

Ⓢ Supporting Information

The Supporting Information is available free of charge on the ACS Publications website at DOI: 10.1021/acs.chemmater.6b00936.

> Additional SEM and TEM images of synthesized NPs and a graph of the dependence of NP shape on experimental parameters in the presence of I^- ions. (PDF)

AUTHOR INFORMATION

Corresponding Author
*E-mail: ekumache@chem.utoronto.ca.

Notes
The authors declare no competing financial interest.

REFERENCES

(1) Roduner, E. Size Matters: Why Nanomaterials are Different. *Chem. Soc. Rev.* **2006**, *35*, 583−592.

(2) Tao, A. R.; Habas, S.; Yang, P. Shape Control of Colloidal Metal Nanocrystals. *Small* **2008**, *4*, 310−325.

(3) Henry, C. R. Surface Studies of Supported Model Catalysts. *Surf. Sci. Rep.* **1998**, *31*, 231−325.

(4) Song, Y.; Hormes, J.; Kumar, C. S. S. R. Microfluidic Synthesis of Nanomaterials. *Small* **2008**, *4*, 698−711.

(5) Li, W.; Greener, J.; Voicu, D.; Kumacheva, E. Multiple Modular Microfluidic (M3) Reactors for the Synthesis of Polymer Particles. *Lab Chip* **2009**, *9*, 2715−2721.

(6) Park, J. Il; Saffari, A.; Kumar, S.; Günther, A.; Kumacheva, E. Microfluidic Synthesis of Polymer and Inorganic Particulate Materials. *Annu. Rev. Mater. Res.* **2010**, *40*, 415−443.

(7) Xie, X.; Gao, G.; Pan, Z.; Wang, T.; Meng, X.; Cai, L. Large-Scale Synthesis of Palladium Concave Nanocubes with High-index Facets for Sustainable Enhanced Catalytic Performance. *Sci. Rep.* **2015**, *5*, 8515.

(8) Klinkova, A.; Cherepanov, P. V.; Ryabinkin, I. G.; Ho, M.; Ashokkumar, M.; Izmaylov, A. F.; Andreeva, D. V.; Kumacheva, E. Shape-dependent Interactions of Palladium Nanocrystals with Hydrogen. *Small* **2016**, DOI: 10.1002/smll.201600015.

(9) Cademartiri, L.; Ozin, G. A. Emerging Strategies for the Synthesis of Highly Monodisperse Colloidal Nanostructures. *Philos. Trans. R. Soc., A* **2010**, *368*, 4229−4248.

(10) Cademartiri, L.; Malakooti, R.; O'Brien, P. G.; Migliori, A.; Petrov, S.; Kherani, N. P.; Ozin, G. A. Large-scale Synthesis of Ultrathin Bi2S3 Necklace Nanowires. *Angew. Chem., Int. Ed.* **2008**, *47*, 3814−3817.

(11) Williamson, C. B.; Nevers, D. R.; Hanrath, T.; Robinson, R. D. Prodigious Effects of Concentration Intensification on Nanoparticle Synthesis: A High-Quality, Scalable Approach. *J. Am. Chem. Soc.* **2015**, *137*, 15843−15851.

(12) Blosi, M.; Albonetti, S.; Ortelli, S.; Costa, A. L.; Ortolani, L.; Dondi, M. Green and Easily Scalable Microwave Synthesis of Noble Metal Nanosols (Au, Ag, Cu, Pd) Usable as Catalysts. *New J. Chem.* **2014**, *38*, 1401−1409.

(13) Cookson, J. The Preparation of Palladium Nanoparticles. *Platin. Met. Rev.* **2012**, *56*, 83−98.

(14) Wang, Y.; Xie, S.; Liu, J.; Park, J.; Huang, C. Z.; Xia, Y. Shape-controlled Synthesis of Palladium Nanocrystals: a Mechanistic Understanding of the Evolution from Octahedrons to Tetrahedrons. *Nano Lett.* **2013**, *13*, 2276−2281.

(15) Brust, M.; Walker, M.; Bethell, D.; Schiffrin, D. J.; Whyman, R. Synthesis of Thiol-derivatised Gold Nanoparticles in a Two-phase Liquid−Liquid System. *J. Chem. Soc., Chem. Commun.* **1994**, *0*, 801−802.

(16) Li, Z.; Gao, J.; Xing, X.; Wu, S.; Shuang, S.; Dong, C.; Paau, M. C.; Choi, M. M. F. Pd Nanoparticles Deposited on Poly(lactic acid) Grafted Carbon Nanotubes: Synthesis, Characterization and Application in Heck C-C Coupling Reaction. *J. Phys. Chem. C* **2010**, *114*, 723−733.

(17) Guerrero-Martínez, A.; Barbosa, S.; Pastoriza-Santos, I.; Liz-Marzán, L. M. Nanostars Shine Bright for You: Colloidal Synthesis,

Properties and Applications of Branched Metallic Nanoparticles. *Curr. Opin. Colloid Interface Sci.* **2011**, *16*, 118−127.

(18) Niu, W.; Zhang, L.; Xu, G. Shape-Controlled Synthesis of Single-Crystalline Palladium Nanocrystals. *ACS Nano* **2010**, *4*, 1987−1996.

(19) Gu, J.; Zhang, Y.-W.; Tao, F. Shape Control of Bimetallic Nanocatalysts Through Well-designed Colloidal Chemistry Approaches. *Chem. Soc. Rev.* **2012**, *41*, 8050−8065.

(20) Niu, W.; Li, Z.-Y.; Shi, L.; Liu, X.; Li, H.; Han, S.; Chen, J.; Xu, G. Seed-Mediated Growth of Nearly Monodisperse Palladium Nanocubes with Controllable Sizes. *Cryst. Growth Des.* **2008**, *8*, 4440−4444.

(21) Chen, Y. H.; Hung, H. H.; Huang, M. H. Seed-mediated Synthesis of Palladium Nanorods and Branched Nanocrystals and their Use as Recyclable Suzuki Coupling Reaction Catalysts. *J. Am. Chem. Soc.* **2009**, *131*, 9114−9121.

(22) Cheong, S.; Watt, J. D.; Tilley, R. D. Shape Control of Platinum and Palladium Nanoparticles for Catalysis. *Nanoscale* **2010**, *2*, 2045−2053.

(23) Deraedt, C.; Astruc, D. "Homeopathic" Palladium Nanoparticle Catalysis of Cross Carbon-carbon Coupling Reactions. *Acc. Chem. Res.* **2014**, *47*, 494−503.

(24) Mubeen, S.; Zhang, T.; Yoo, B.; Deshusses, M. A.; Myung, N. V. Palladium Nanoparticles Decorated Single-Walled Carbon Nanotube Hydrogen Sensor. *J. Phys. Chem. C* **2007**, *111*, 6321−6327.

(25) Liu, S.; Tang, Z. Nanoparticle Assemblies for Biological and Chemical Sensing. *J. Mater. Chem.* **2010**, *20*, 24−35.

(26) Lim, S. H.; Wei, J.; Lin, J.; Li, Q.; KuaYou, J. A Glucose Biosensor Based on Electrodeposition of Palladium Nanoparticles and Glucose Oxidase onto Nafion-solubilized Carbon Nanotube Electrode. *Biosens. Bioelectron.* **2005**, *20*, 2341−2346.

(27) Yu, H.; Ma, Z.; Wu, Z. Immobilization of Ni−Pd/core−shell Nanoparticles through Thermal Polymerization of Acrylamide on Glassy Carbon Electrode for Highly Stable and Sensitive Glutamate Detection. *Anal. Chim. Acta* **2015**, *896*, 137−142.

(28) Li, G.; Kobayashi, H.; Taylor, J. M.; Ikeda, R.; Kubota, Y.; Kato, K.; Takata, M.; Yamamoto, T.; Toh, S.; Matsumura, S.; Kitagawa, H. Hydrogen Storage in Pd Nanocrystals Covered with a Metal−organic Framework. *Nat. Mater.* **2014**, *13*, 802−806.

(29) Yamauchi, M.; Ikeda, R.; Kitagawa, H.; Takata, M. Nanosize Effects on Hydrogen Storage in Palladium. *J. Phys. Chem. C* **2008**, *112*, 3294−3299.

(30) Xia, Y.; Xiong, Y.; Lim, B.; Skrabalak, S. E. Shape-Controlled Synthesis of Metal Nanocrystals: Simple Chemistry Meets Complex Physics? *Angew. Chem., Int. Ed.* **2009**, *48*, 60−103.

(31) Yoo, S.-H.; Lee, J.-H.; Delley, B.; Soon, A. Why does Bromine Square Palladium Off? An ab initio Study of Brominated Palladium and its Nanomorphology. *Phys. Chem. Chem. Phys.* **2014**, *16*, 18570.

(32) Zhang, J. A.; Langille, M. R.; Personick, M. L.; Zhang, K.; Li, S. Y.; Mirkin, C. A. Concave Cubic Gold Nanocrystals with High-Index Facets. *J. Am. Chem. Soc.* **2010**, *132*, 14012−14014.

(33) Zhang, Q.; Zhou, Y.; Villarreal, E.; Lin, Y.; Zou, S.; Wang, H. Faceted Gold Nanorods: Nanocuboids, Convex Nanocuboids, and Concave Nanocuboids. *Nano Lett.* **2015**, *15*, 4161−4169.

(34) Yu, Y.; Zhang, Q. B.; Xie, J. P.; Lee, J. Y. Engineering the Architectural Diversity of Heterogeneous Metallic Nanocrystals. *Nat. Commun.* **2013**, *4*, 1454−1462.

(35) Niu, W.; Zhang, W.; Firdoz, S.; Lu, X. Controlled Synthesis of Palladium Concave Nanocubes with Sub-10-Nanometer Edges and Corners for Tunable Plasmonic Property. *Chem. Mater.* **2014**, *26*, 2180−2186.

(36) Fan, F. R.; Liu, D. Y.; Wu, Y. F.; Duan, S.; Xie, Z. X.; Jiang, Z. Y.; Tian, Z. Q. Epitaxial Growth of Heterogeneous Metal Nanocrystals: From Gold Nano-octahedra to Palladium and Silver Nanocubes. *J. Am. Chem. Soc.* **2008**, *130*, 6949−6951.

(37) Lu, F.; Tian, Y.; Liu, M.; Su, D.; Zhang, H.; Govorov, A. O.; Gang, O. Discrete Nanocubes as Plasmonic Reporters of Molecular Chirality. *Nano Lett.* **2013**, *13*, 3145−3151.

(38) Klinkova, A.; Ahmed, A.; Muntyanu, A.; Gang, O.; Walker, G. C.; Kumacheva, E.; et al. Structural and Optical Properties of Self-Assembled Chains of Plasmonic Nanocubes. *Nano Lett.* **2014**, *14*, 6314−6321.